International Journal of Energy
ISSN: 2957-9473 | Vol. 4, No. 3, 2024

Background Noise Imaging-based Monitoring of Water-driven Leading Edges

Feng Yang *

Sinopec with Research Institute of Petroleum Engineering Technology, Sinopec Shengli Oilfield Company, Dongying Shandong, 257000, China

*** Corresponding author Email:** yangfeng716.slyt@sinopec.com

Abstract: This paper investigates the necessity of monitoring the leading edge of water drive in the process of compression drive, and points out the limitations of the existing technology, among which the microseismic monitoring method is less costly and widely used but less accurate. Tracer tracking is reliable, and water injection effect can be judged by monitoring tracers in production wells, but the operation and interpretation are more cumbersome. Four-dimensional time-shifted seismic monitoring is reliable and can determine the location of water-driven front and predict the distribution of residual oil in long-term water-driven reservoirs, but the cost is high, the cycle time is long and the acquisition is inconsistent. And a new technique based on passive source time-shift imaging is proposed, which is based on background noise imaging with autocorrelation seismic interferometry to realize low-cost and long-time water-drive leading edge monitoring. The experimental results show that the way and number of geophones are deployed directly affect the imaging effect, in which the performance of the wire-bundle-like observation system is better than that of the ring-like system, and the more the number of geophones, the better the imaging effect. Effective dynamic monitoring of the water-driven leading edge was carried out in two mines using this technology, confirming its stability and reliability in practical application. The study provides a complete set of monitoring process, which brings the possibility of technology optimization for future oilfield development, and suggests combining with microseismic monitoring to improve the imaging accuracy and monitoring effect.

Keywords: Water Drive Leading Edge Monitoring; Passive Source Time-shift Imaging; Background Noise Imaging; Autocorrelation Seismic Interferometry; Dynamic Monitoring; Microseismic Monitoring.

1. Introduction

The monitoring of water-driven leading edge of injection wells is of great significance for optimizing the later injection and production network, tapping the residual oil potential, and improving the final recovery rate. The monitoring of water-driven leading edge is the key research content of Sinopec's scientific and technological research project "Pilot test and application of pressure-driven technology in low-permeability reservoirs". However, during the process of pressure-driven water injection, the changes of pressure-driven cracks and water-driven leading edge of producing wells are not clearly recognized. Although microseismic monitoring, tracers and four-dimensional seismic are widely used, it is difficult to balance their reliability and cost. Therefore, research on real-time and low-cost methods for continuous monitoring of water-driven leading edge has important application and economic value.

Currently, commonly used monitoring methods include microseismic monitoring, tracer tracking and four-dimensional time-shift seismic monitoring. The microseismic monitoring method is low-cost, but the accuracy is low; the tracer tracking method is reliable, but the operation is complicated; the four-dimensional time-shift seismic monitoring method is able to predict the distribution of residual oil in long-term water-driven reservoirs, but the cost is high and the period is long. With the wide application of nodal meters, it has become possible to realize long-time monitoring by continuously acquiring background noise. This method has the advantages of low cost and long time monitoring by acquiring the background noise generated during the long time pressure drive process and monitoring the changes of the water drive leading edge surface by using the time-shift passive source imaging method.

The in-depth study of water-driven leading edge monitoring technology based on time-shift imaging of passive sources is not only of important research value, but also of practical application significance. This test is aimed at predicting the subsurface pressure-driven leading edge surface of production wells under pressure-driven, which provides an important basis for subsequent production and development. This work not only provides practical reference for field construction, but also provides technical support and guidance for the efficient development of the oilfield and the increase of reserves and production.

2. Background Noise Imaging Technique and Its Test Method

2.1. Background Noise Imaging Theory

2.1.1. Basic Principles of Seismic Interferometry

Seismic interferometry is the basis of passive source imaging, and currently, the interferometric algorithms for processing background noise data are: mutual correlation, inverse plethysmography, mutual stemming, and autocorrelation methods.

The mutual correlation is actually the seismic interferometry extracted Green's function through the background noise mutual correlation acquired by the geophone. The specific formula is:

$$H(f) = \left| P(f)^2 \right| G(x_A, f) G^*(x_B, f) \quad (1)$$

where the seismic source function is assumed to be

$P(f)$, The Green's function for the two checkpoints at point A and point B is $G(x_A, f)$ and $G(x_B, f)$.

When the two selected geophones are progressively closer to merging into a single point, the cross-correlation expression can then be expressed as an autocorrelation function of the single-channel data:

$$H(f) = P(f)^2 G(x, f)^2 \quad (2)$$

Unlike the cross-correlation method, which recovers the reflected signal between two geophones, the autocorrelation method recovers the self-excited self-recovery record of a single geophone through the autocorrelation of the receiver noise record of the subsurface seismic source, which in turn establishes the reflected wave profile. In practice, due to the quality of the data, it is sometimes difficult to recover a false gun set record that can be used for subsequent imaging. Therefore, the use of background noise autocorrelation to obtain the subsurface body wave reflection signal is a great supplement for passive source seismic interferometric imaging, and the subsequent profile imaging processing of this test finally adopts the autocorrelation method.

2.1.2. Background Noise Passive Time-shifted Seismic Method Realization Flow

In the actual data processing, this test divides the background noise passive time-shifted seismic method into three steps.

The first step is data preprocessing. Passive source seismic exploration requires continuous acquisition of a large amount of data, so it is necessary to cut the continuous data by a fixed length, and then arrange the panel data according to the offset distance. The length of the cut needs to be moderate, too short or too long will affect the imaging effect. The preprocessing steps include removing the mean, linear trend, and instrument response, followed by spectral analysis, bandpass filtering, and normalization, and finally filtering to retain the useful body wave signals.

The second step is imaging. The passive source profile is extracted by autocorrelation of background noise, which directly characterizes the structural distribution of the subsurface stratigraphy, equivalent to a self-excited self-recovery profile.

The third step is time-shifted seismic. Data from different time periods are selected for imaging, and by comparing the changes in the dummy profile data, the dynamic change characteristics of subsurface fluid transport and water-driven leading edge are obtained for dynamic monitoring.

2.2. Test of Data Acquisition Methods for Pressure-driven Passive Sources

The forward simulation method is used to experiment with different observing system designs, to optimize the best nodal geophone arrangement and system parameters according to the monitoring objectives, and to carry out 2 sets of actual observations. Ten groups of different noise theoretical models are established, and noise record synthesis and processing tests are carried out to analyze and verify the feasibility of the method.

2.2.1. Typical Noise Theory Model Test

The synthetic records and processing results of 10 groups of different models are tested to verify the feasibility of the method for water-driven leading edge. In order to test the influence of different seismic source distributions on the imaging results and verify the possibility of monitoring the water-driven leading edge, 6 typical models with different seismic source distributions and those conforming to the actual seismic source distributions were firstly established, and the data were collected by the forward simulation for the next step of processing and analysis. Then, 4 typical models of different locations of the water injection leading edge, which conform to the actual seismic source distribution, were established, and the data were collected by forward simulation for further processing and analysis.

In this test, different models were produced mainly by adjusting the geophone position, the wave and position of the leading edge of the injection front, and the descending speed. A total of random seismic source before water injection, two side seismic source models before water injection, shallow seismic source model before water injection, middle seismic source model before water injection, bottom seismic source model before water injection, water injection front fit to the actual model, water injection descending speed 150m/s wave and 600m model, water injection descending speed 1000m/s wave and 400m model, water injection descending speed 1000m/s wave and 600m model, and water injection descending speed 1000m/s wave and 800m model. (Only the first four sets of test results are shown in this paper, and the corresponding imaging results are shown in Fig. 1.)

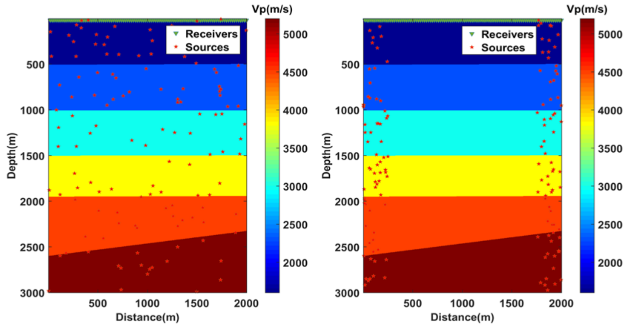

(a) stochastic seismic source modeling before water injection

(b) modeling of seismic sources on both sides before water injection

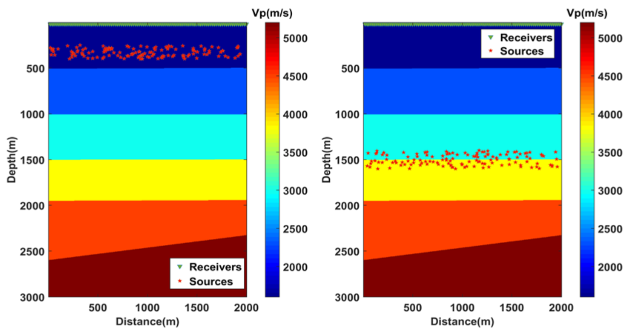

(c) modeling of shallow seismic sources before water injection

(d) modeling of the central seismic source before water injection

Figure 1. Noise Theory Model

Active-source forward simulations are performed for the 10 noise models, and 10 active-source single-gun records are obtained. From Fig. 2, it can be seen that a new reflection axis appears around 1.2s, which is caused by the strong reflection coefficient appearing in the velocity decrease of the formation, and the larger the velocity decrease, the more obvious the difference is. The moment of the appearance of this same-phase axis coincides with the design of the water injection model, and at the same time, the seismic wave velocity reduction will lead to the occurrence of the same-phase axis of the downward pull phenomenon, so that the data below in the phase will be changed, resulting in the velocity change before and after the same-phase axis can not be aligned. From the red box, it can be seen that the more drastic changes in the subsurface occur, the more obvious the seismic response is, which is favorable for later monitoring.

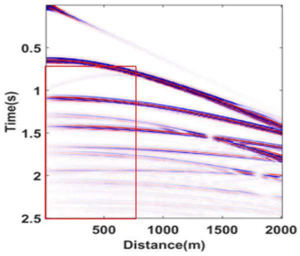

(a) Pre-injection model active source single gun

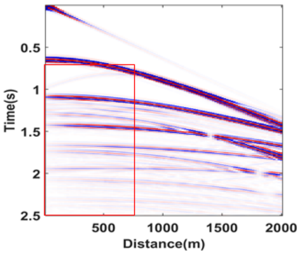

(b) Water injection down speed 150m/s wave and 600m active source single gun

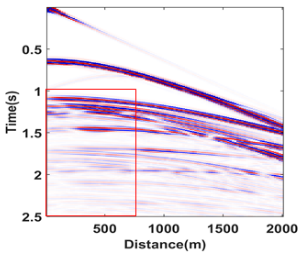

(c) Water injection down speed 1000m/s wave and 400m active source single gun

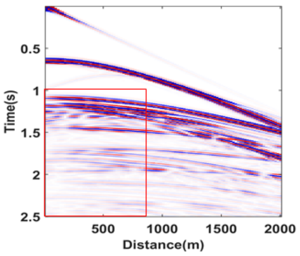

(d) Water injection down speed 1000m/s wave and 600m active source single gun

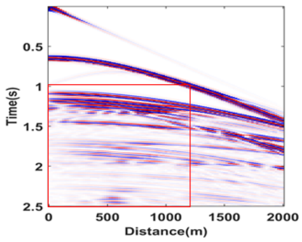

(e) Water injection down speed 1000m/s wave and 800m active source single gun

Figure 2. Active Source Single Cannon

In order to test the effect of different source distributions on imaging results and active source single-gun comparison, a passive source seismic record of 10 min length is simulated by the passive source observation system for 10 noise models, and the virtual gun sets obtained after a series of passive source interferometry processing processes. The quality of the reconstructed false gun sets with noise signals is obviously reduced, and by comparison, the more random and downward the distribution of seismic sources, the more obvious the single gun response of the reconstructed false gun sets, and the tested close to the actual model meets the needs of practical monitoring, and the difference of the seismic response of the leading edge of the water drive is obvious. In addition to this, the dummy gun sets with different changes in velocity after liquid injection can be seen in the red box with the same results as the active source, and a new reflection axis appears around 1.2 s. The larger the descending velocity is, the more obvious the difference is, which is the seismic response caused by the change in the position of the water injection leading edge, and the feasibility of the method is verified.

In order to test the possibility of background noise imaging to monitor the water-driven leading edge, noise data from different water-driven leading edges before and after water injection are imaged. It can be found that the imaging quality of the model with poorer quality of reconstructed virtual cannon set is also poorer, and the new isophase axis appearing near 1.2 s after water injection for the model that conforms to the actual seismic source distribution is more similar to the location and morphology of velocity anomalies designed in the water injection model, which can respond to the changes in the reservoir before and after water injection.

In order to better highlight and monitor the changes in the target layer, the imaging profiles before and after the water injection from passive sources, which conform to the actual seismic source distribution, are processed by mutual homogenization and displayed in the order of geophones. From the red box, it can be clearly observed that the homoclinic axis of the target layer is mis-segmented, and the continuity of the homoclinic axis above the target layer is better, which can be inferred that the stratigraphy in this section has changed drastically, providing a basis for monitoring the leading edge of the water drive.

Since the actual passive source body wave data obtained are usually low-frequency, in order to better demonstrate the transportation of the water-driven leading edge and eliminate other interferences, F-X and low-pass filtering are applied to the imaging results to obtain the final imaging results. It is obvious that different wave ranges of the water-driven leading edge surface can be obtained, so as to realize the dynamic monitoring of the water-driven leading edge surface.10 sets of theoretical experimental results show that it is feasible to use the passive source imaging for time-shift monitoring. This results in a process of processing and interpretation of background noise imaging for monitoring the water-driven leading edge.

2.2.2. Experiments on The Effect of The Number of Detectors and Observation Mode on Imaging

In this paper, the effects of different numbers and deployment methods of geophones on the imaging effect are analyzed by an indoor forward simulation method. The tests were set up with 400, 300, 200, 150-line bundle-like and 200, 100 ring-like, and a total of six groups of tests were conducted. (Only the first two groups of test results are shown in this paper, and the corresponding imaging results are shown in Fig. 3.)

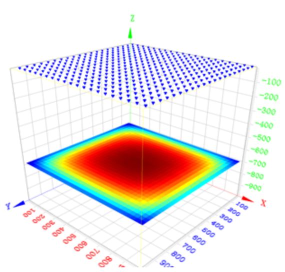

(a) 500 geophones beam-like observation system and imaging effect

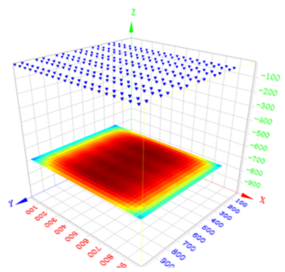

(b) 300 geophones beam-like observation system and imaging effect

Figure 3. Observing System Design Analysis

Comparative analysis reveals that the imaging quality gradually decreases as the number of geophones decreases, and that the imaging effect of the wire-bundle-like observation system is better than that of the ring-like system. The imaging effect of the wire-bundle-like system can meet the monitoring needs, especially when the geophones are arranged near the location that needs to be imaged. In order to monitor the progress of the water-driven leading edge surface, it is recommended to use a distributed wire-bundle-like system to balance the acquisition cost and imaging quality. If there are enough geophones on site, it is recommended to deploy a densely arranged harness-like observation system as shown in Figure 3(a), which can monitor the water drive leading edge from multiple angles. In this test, two wells were designed according to the actual construction situation.

In summary, the test results show that reducing the number of geophones reduces the imaging quality, and that a harness-like observation system is more effective than a ring-like system. In order to monitor the water-driven leading edge surface, it is recommended to use a distributed harness-like (radial) observation system to balance the imaging quality and cost. If conditions permit and there are enough geophones, a densely arranged beam system is recommended.

Through 10 sets of theoretical modeling experiments, the more drastic changes occurring in the subsurface are more favorable for monitoring, which provides a basis for monitoring changes in the water-driven leading edge, verifies the possibility of using background noise imaging for monitoring the water-driven leading edge, and obtains the technical route for monitoring the water-driven leading edge based on background noise imaging as shown in Fig. 4.

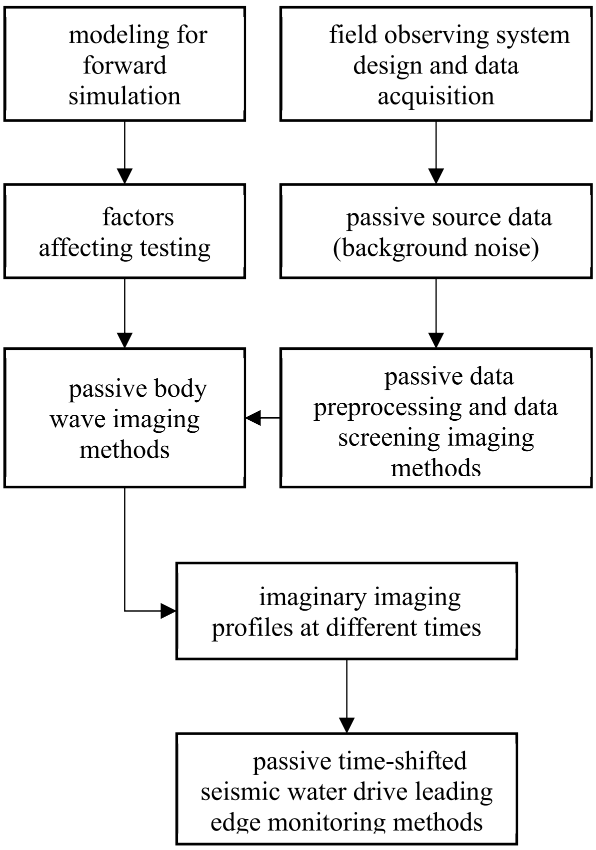

Figure 4. A Technical Route for Monitoring the Leading Edge of Water Drives Based on Background Noise Imaging

2.3. Experimentation with Imaging Processing Methods for Noise Data

2.3.1. Methodological Theory

The actual acquired noise data are significantly different from the theoretical data, and a series of complex processing is required to accurately reconstruct the empirical Green's function. The processing flow of the seismic interferometry-based passive source method includes data preprocessing, seismic interferometry processing, and time-domain superposition. The preprocessing steps (e.g., de-mean, de-trending, resampling, band-pass filtering, etc.) are key to improving the quality of the superimposed results. Imaging can be significantly improved by segmenting and stacking long-time noise records, but data need to be screened to avoid noise swamping the effective signal. Key denoising algorithms include F-K filtering, F-X filtering, spectral whitening, etc. Illumination diagnostic algorithms for body-wave screening determine whether the relevant noise panel is dominated by body waves by selecting ray parameter limits based on expected body and surface wave velocities. Since body waves are usually faster than surface waves, the energy peaks of body waves generally occur in the smaller slowness range, whereas surface waves occur in the larger slowness range, and thus noise fragments containing body wave information can be retrieved.

2.3.2. Data Preprocessing Tests

The actual acquired background noise data differs greatly from the theoretical noise data and contains very little valid signal that can be used directly for imaging. Pre-processing is required for further imaging. Twenty sets of tests with different denoising methods were performed for different noise problems.

By adjusting the filtering band parameters to test, five groups of different filtering band test results show that band-pass filtering can eliminate part of the low-frequency and high-frequency noise, improve the data signal-to-noise ratio, after the test when the filtering band 0-20-30-40Hz when the best results.

Tested by adjusting the visual speed parameter, the test results of five groups of different visual speed selection show that F-K filtering can eliminate part of the surface wave noise, with the increase of the visual speed selection, the more noise is removed, and may remove part of the effective signal, after testing when the visual speed is 850m/s the best effect.

Over the adjustment of the filter length and whitening factor parameters to test, five groups of different filter length and whitening factor test shows that the practical application of the comprehensive consideration of the calculation speed and effect, filter length 20 whitening factor 0.1 when the removal of random noise, fixed-frequency noise, enhancement of the effective signal is the best effect. The longer the filter length, the worse the effect, and the whitening factor has less effect on the results.

By adjusting the time window parameters for testing, the spectral whitening test results of 5 groups of different time windows show that, in practical applications, taking into account the calculation speed and effect, it is more appropriate to choose a time window of about 20, which can effectively broaden the data band to improve the resolution. With the increasing time window selection, the data resolution decreases.

2.3.3. Data Screening Tests

Data preprocessing can improve the signal-to-noise ratio of the data, but the mixing of surface and body wave frequencies makes it difficult to discriminate body wave signals. In order to screen out the body wave segments that are favorable for imaging, 10 sets of data screening tests were conducted, and 5 sets of noisy time segments that need to be discarded and 5 sets of time segments containing body waves that need to be retained were successfully screened out. The proposed screening algorithm performs stably and feasibly in real data tests, and can effectively distinguish body waves from other data.

2.3.4. Imaging Method Testing

Noisy data are imaged using different methods, using different time length data imaging, integrated imaging accuracy and efficiency, optimize the most suitable imaging method, and improve the imaging process. After 10 groups of imaging methods are tested, the longer the time of data acquisition, the more accurate the imaging, in which the autocorrelation imaging is the fastest efficiency, and can achieve good results. However, in the actual data imaging, the other three methods are difficult to accurately image, poor noise immunity, the actual imaging using autocorrelation method.

2.3.5. Summary

Data preprocessing removes most of the noise, and then data screening can greatly improve the quality of the imaging data and the accuracy of the imaging results. This results in a set of processes for processing real noise data as shown in Figure 5.

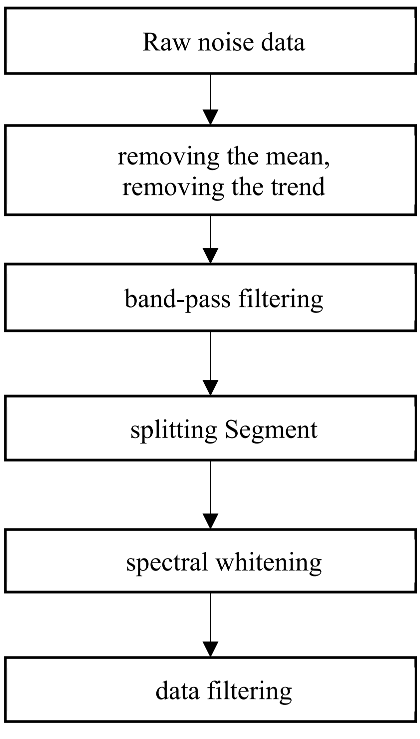

Figure 5. Actual Noise Data Processing Flow

In the actual data imaging, the longer the data collection time the more accurate imaging, autocorrelation imaging is the most efficient, good imaging effect and has a strong noise immunity, so the actual imaging using autocorrelation method.

3. Methods of Interpreting Noise Imaging Results for Pressure-driven Monitoring

After completing the testing of the passive source data acquisition method and the noise data imaging processing method, we formed the technical process of water-driven leading edge monitoring based on background noise imaging. In order to realize low-cost dynamic monitoring of the water-driven leading edge surface, interpretation of the water-driven leading edge surface, fracture interpretation, and prediction of the direction and intensity of fracture development in the range of water-injection wells and production wells, we tested the data acquisition of the observation system design, data preprocessing, and the noise imaging results compression-driven monitoring and interpretation method on the actual well site.

3.1. Dynamic Monitoring Test of Water-driven Leading Edge Surface

During the implementation of pressure-drive in the actual A well, the underground reservoir pressure-drive front is monitored in real time by ground passive source seismic monitoring technology, and the microseismic activity during the water-drive process is recorded. The monitoring data are processed and interpreted, and the pressure-drive front is mapped. Monitor microseismic and other events by deploying geophones on the ground to ensure that the equipment is technically sound. Monitoring underground reservoir imaging in the whole process, providing changes in the pressure-drive front, and providing basis for evaluating the pressure-drive effect and later development.

Monitoring detector station equipment coverage length design: monitoring detector station equipment to a water injection well inclined well bottom horizontal projection as the center to the production wells well bottom horizontal projection between the deployment, the envelope radius of 350-400 m. Monitoring detector station equipment buried position design: the use of harness-like observation, a total of trenching and burying 7 lines, a total of 49 sets of shallow buried equipment, the detector interval of 50m.

Passive source seismic acquires the weak vibrations generated during underground reservoir development. The vibrations induced during the water drive process have huge energy differences and a wide frequency range. In order to image the underground reservoir and analyze the changes of the water-driven front surface, it is necessary to acquire the vibration signals continuously for a long time. This time, a node-type geophone capable of continuous acquisition for more than 20 days was used to realize uninterrupted monitoring of the signals.

According to the processing flow obtained from the test, the collected data are preprocessed to eliminate various interferences. The data are then screened to use a direct imaging algorithm for nodal reflected waves based on interference theory. For unstable passive source signals, signal differences in the imaging profile that are not related to reservoir changes need to be eliminated before time-shift analysis can be performed. According to the task requirements, a time-shift analysis of the pressure-driven monitoring signals is performed to determine the reservoir differences. This analysis requires at least two imaging sessions, with the number of imaging sessions proportional to the accuracy required.

The filtered noise data and valid data containing body waves will be used for subsurface reservoir monitoring using passive source imaging methods.

Results of the phase I imaging discrepancy monitoring:

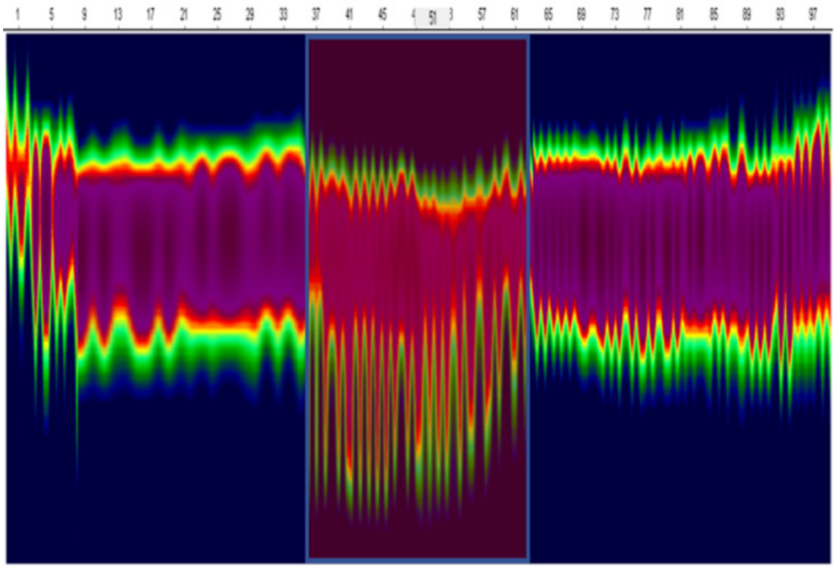

Figure 6. Noise Imaging Time-shift Data Effects (Initial vs. Pre-imaging Difference Data)

Figure 6 shows the monitoring comparison results of the data collected 18 days before the start of the compression drive project (2023.12.27-2024.2.15). Figure 7 shows the monitoring results from the beginning to the end of the compression drive project (2023.12.27-2024.2.15). From the test results, it can be concluded that the compression drive has affected the underground reservoir, and by projecting the locations with large differences in the imaging onto the corresponding geophone locations, we can clearly observe the areas of change in the subsurface, and thus obtain the water-driven leading edge surface.

Phase II imaging discrepancy monitoring results:

The subsurface pressure drive predicted by the passive source imaging method for a total of 37 days, from 2023.12.27 to 2024.02.04, is illustrated in Figure 7. The fracture distribution in the figure is predicted by the monitoring situation.

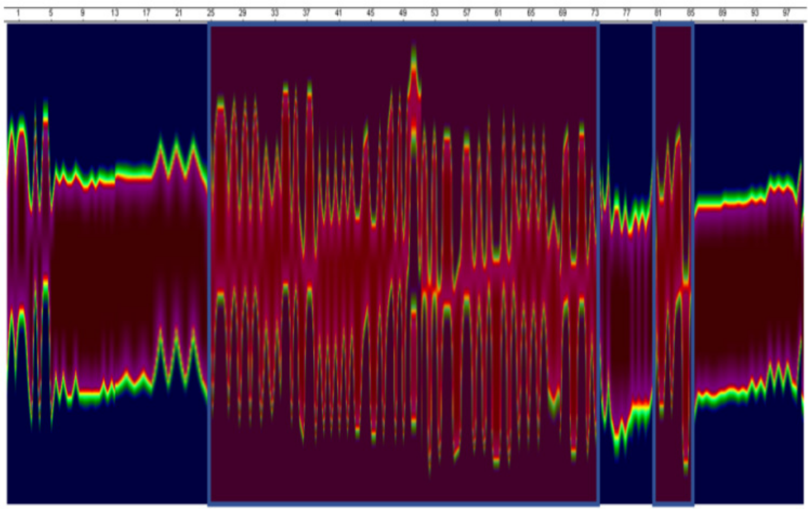

Figure 7. Noise Imaging Time-shift Data Effects (Initial vs. Post Imaging Differences)

A total of 37 days of background noise vibration data were collected for this pressure-driven monitoring. These data were imaged three separate times, and the differences between the two imageries were compared. It was analyzed that the compression drive surface continued to advance as the compression drive proceeded, and good results were achieved. One of the wells has the smallest reservoir change, showing that the pressure-driven surface is advancing forward under the pressure-driven effect, but the resistance is high. It is recommended that further compression drive operations be carried out on this well, and with the advancement of the compression drive surface, it is expected that there will be a very significant increase in production.

3.2. Summary

Through the technical route and actual noise processing flow of water drive leading edge monitoring with background noise imaging formed in the previous paper, the water drive leading edge monitoring work was carried out in the actual work area. From the monitoring results, the proposed method can effectively monitor the water-driven leading edge surface, and can provide scientific guidance for the optimization of oilfield development technology and other work.

4. Conclusion

The following conclusions and insights have been gained from the testing work that has been done:

(1) The test results for pressure-driven passive source data acquisition and processing methods show that the proposed method verifies the feasibility of background noise imaging for water-driven leading edge monitoring. Different acquisition methods, number of geophones, and different source distributions will affect the imaging effect; compared with theoretical data, the preprocessing and screening of actual data are crucial.

(2) Based on the actual collected passive source signals and passive source noise time-shift imaging technology, we have completed the application test of dynamic monitoring of actual water-driven leading edge surface based on ground-based nodal instrument, and formed the crack interpretation method based on dynamic monitoring of water-driven leading edge. Theoretical and practical data experiments show that the proposed method is stable and reliable, and can better monitor the dynamic changes of the water-driven leading edge, and has good practical value.

(3) In view of the current situation of time-shift monitoring of passive sources, it is suggested that joint monitoring work based on microseismic and noise time-shift imaging can be carried out. At the same time, the imaging difference should be further enhanced, and the arrangement of the observation system should be appropriately encrypted under the condition, so as to make the cutting-off surface of the water drive leading edge clearer and better highlight the transportation situation of the leading edge surface of the water drive.

Acknowledgments

In the research process of this project, we have received great support and help from leaders and experts of various departments such as Shengli Engineering Institute! During the project opening and research stage, the group of experts put forward many constructive comments and suggestions on the related research, and we would like to express our sincere thanks for them!

References

[1] Zhu Heng, Wang Deli, Shi Zhian, et al.Passive seismic imaging of seismic interferometry[J].Progress in Geophysics, 2012,27 (2): 496-502.

[2] Zhang Pan, Han Liguo, Liu Qiang, et al.Interpolation of seismic data from active and passive sources and their joint migration imaging[J]. Chinese Journal of Geophysics, 2015, 58(4):1754-1766.

[3] Fang Jie, Yan Haofei, Liu Guofeng.Passive seismic body wave extraction technology and it's quality control[J]. Progress in Geophysics,2019,1-15.

[4] Liu Guofeng, Liu Yu, Meng Xiaohong, et al.Surface wave and body wave imaging of passive seismic exploration in shallow coverage area application of Inner Mongolia[J]. Chinese Journal of Geophysics,2021,64(3):937-948.

[5] Guo Xin, Zou Zhihui.Numerical Study of Passive Time-lapse Seismic Method[J]. Chinese Journal of Engineering Geophysics, 2023, 20(4):518-528.

[6] Gan Lideng, Yao Fengchang, Du Wenhui, et al.4D seismic technology for water flooding reservoirs[J]. Petroleum Exploration and Development,2007,34(4):437-444.

[7] Rui Yongjun. Key processing technique for land non-uniform acquisition of time-lapse seism[J]. Geophysical and Geochemical Exploration,2016, 40(4):778-782.

[8] Lei lei. Rock physical analysis and seismic forward modeling for CO_2 flooding[J]. Progress in Geophysics,2016,31(2):675-682.

[9] You Rongjun, Yan Zhaotao. The applicability of time-lapse seismic monitoring in the geological storage of CO_2[J]. Computing Techniques For Geophysical and Geochemical Exploration,2016,38(3):1001.

[10] M.D. Jackson, A.H. Muggeridge, Imperial College.Effect of Discontinuous Shales on Reservoir Performance During Horizontal Waterflooding[J].SPE Journal,2000,Vol.5(4): 446-455.

[11] Jupe A, Cowles J. Microseismic monitoring: listen and see the reservoir [J]. World Oil, 1998, 219(12) : 171-174.

[12] Yiqiang L. Experimental Study on Physical Simulation of Polymer Flooding Large Plane Model. Beijing, China: Graduate University of Chinese Academy of Sciences; 2006.

[13] Chuanfeng Z, Hanqiao J, Minfeng C, et al. Waterflooding state law of fractured sandstone reservoirs. J Xi'an Shiyou Univ (Natural Science Edition). 2006;02:26-28+4.

[14] Wang Chunsheng,Sun Zexin, Sun Qiji, et al.Comprehensive evaluation of waterflooding front in low-permeability reservoir.[J].Energy Science & Engineering,2021,Vol.9(9): 1.

[15] Ivandic M, Bergmann P, Kummerow J, et al. Monitoring CO2 saturation using time-lapse amplitude versus offset analysis of 3D seismic data from the Ketzin CO2 storage pilot site, Germany[J]. Geophysical Prospecting, 2018, 66, 8:1568-1585.

[16] Zhao Xianzheng, Deng Zhiwen, Bai Xuming, et al. Environmental protection seismic exploration technology and application in grassland area of Erlian Basin [J]. Oil Geophysical Prospecting, 2015, Vol.50 (1): 14-19,13.

[17] Yunshan Lei, Hongxiao Ning, Hu Xiao, et al. Joint application of node and wired instrument in high altitude mountain area [A].2018 SEG International Exposition and Annual Meeting [C],2018.

[18] Bensen G D, Ritzwoller M H, Barmin M P, et al. Processing seismic ambient noise data to obtain reliable broad-band surface wave dispersion measurements[J]. Geophysical Journal International, 2007, 169(3):1239-1260.

[19] Vidal C. Almagro, Draganov D, Vander Neut, et al. Retrieval of reflections from ambient noise using illumination diagnosis. Geophysical journal international, 2014, 198(3): 1572-1584.

[20] Michał Chamarczuk, Michał Malinowski, Yohei Nishitsuji, et al. Automatic 3D illumination-diagnosis method for large- N arrays: Robust data scanner and machine-learning feature provider. Geophysics, 2019, 84(3): Q13-Q25.

[21] Jie Fang, Yu Liu, Guofeng Liu.Enhancing body waves in passive seismic reflection exploration: A case study in Inner Mongolia, China[J].Interpretation,2022,Vol.10(2): B13-B24.

[22] GU, Ning, CHAMARCZUK Michal, GAO Ji, et al.Passive Seismic Structure Imaging of a Coal Mine by Ambient Noise Seismic Interferometry on a Dense Array.[J].Acta Geologica Sinica, 2021, 95: 37-39.

[23] Liu Guofeng, Liu Yu, Meng Xiaohong, et al. Surface wave and body wave imaging of passive seismic exploration in shallow coverage area application of Inner Mongolia [J]. Journal of Geophysics, 2021, 64 (3): 937-948.

[24] Fengjiao Zhang, Zhuo Xu, Christopher Juhlin, et al.Passive seismic interferometry imaging: An example from the Ketzin pilot CO2 geological storage site[J].Journal of Applied Geophysics,2022, 205: 104765.

[25] Thorbecke J W, Draganov D. Finite-difference modeling experiments for seismic interferometry[J]. Geophysics, 2011, 76(6):H1-H18.